JOURNAL OF MATERIALS SCIENCE: MATERIALS IN MEDICINE 9 (1998) 463–473

Morphological and mechanical study on the effects of experimentally induced inflammatory knee arthritis in rabbit long bones

QIAN KANG, Y. H. AN*, H. F. BUTEHORN III, R. J. FRIEDMAN
Orthopaedic Research Laboratory, Department of Orthopaedic Surgery Medical University of South Carolina, Charleston, SC 29425, USA
E-mail: anh@musc.@edu

Inflammatory knee arthritis was induced by intraarticular injection of carrageenan twice a week for a total of 6 weeks in New Zealand White rabbits and the effects of the arthritis on the morphological and mechanical properties of the adjacent femur and tibia were evaluated 8 weeks after the first injection. Carrageenan-induced knee arthritis resulted in severe osteopenic changes and a dramatic decrease in bone strength of the entire ipsilateral femur and tibia, including the femoral head and distal tibia, but not the contralateral femur and tibia and the remote humerus. The osteoporotic changes of the adjacent bones of the inflammatory arthritic knee are the basis for the reduced mechanical strength of these bones. These findings may have clinical significance with regard to the mechanisms and consequences of osteoporotic changes in patients with rheumatoid arthritis.

1. Introduction

Although carrageenan arthritis has been created in rats as a multiarthritis model and in larger animals such as rabbits or dogs as single arthritis model, the effects of carrageenan arthritis on the morphological and mechanical properties of the adjacent long bones has not been well studied. Bogoch *et al.* [1–4] reported that carrageenan-induced knee arthritis caused juxtaarticular osteopenia to the adjacent femoral metaphyseal and diaphyseal bone in a rabbit model. Søballe *et al.* [5] reported a dog model in which the femoral condyle was characterized using morphological and mechanical test methods.

The mechanical properties of osteopenic bone are also very important parameters in osteoporotic conditions, fracture mechanics, or bone ingrowth to prosthetic surfaces under osteopenic conditions. Although this osteopenic model has been characterized morphologically to a certain degree, there has been only one report evaluating the mechanical properties of osteopenic bone, that being in the distal femoral condyle of the dog by indentation testing only [5].

Bone mass is known to decrease in the absence of stimulation from gravity or weight-bearing ambulation [6–9], therefore the "leg disuse" phenomenon commonly found in this model may play an important role in the pathogenesis of the osteopenia. Several other factors, such as interleukin 1 and prostaglandin E [2, 4], changes in local blood flow due to increased intraarticular pressure [10], and the presence of a joint effusion [11] resulting from the arthritis, have been considered to be important for the pathophysiological mechanism of this osteopenia, but all of them lack sound evidence. Questions still remain, such as are there any structural or morphological changes in the proximal femur and the tibia or the humerus for all of the epiphyseal, metaphyseal and diaphyseal area? Are there any changes of mechanical properties of these bones? Are there any morphological and mechanical changes of the bones at remote locations such as the controlateral femur or tibia or both humeri? What are the relationships between the morphological and mechanical changes?

The hypothesis of this study is that if the "disuse" theory is true, carrageenan-induced inflammatory knee arthritis would cause osteopenia to the whole femur and tibia on the arthritis side and consequently result in diminished mechanical strength to these bones, but not to the contralateral femur and tibia or the humerus. To verify the hypothesis, inflammatory knee arthritis was induced by intraarticular injection of carrageenan in adult rabbits on the right side and the effects of the arthritis on the morphological and mechanical characteristics of the adjacent bones (right femur and tibia) and the remote long bones (contralateral femur and tibia and both humeri) for both the cancellous and cortical portions of the bone were evaluated.

2. Materials and methods

2.1. Animals

Adult male New Zealand White rabbits (4.0 ± 0.5 kg) were used. Based on the studies by Gardner [12] and

*Author to whom all correspondence should addressed.

0957–4530

Bogoch *et al.* [1–3], it was necessary to inject 1% carrageenan at intervals of not more than 7 days to produce a prolonged arthritis. In this study, all of the right knee joints of 36 rabbits were injected with 0.3 ml 1% carrageenan twice a week for 6 weeks. No injections were given into the left knee. At 2 weeks after the first injection, titanium cylindrical implants (8.0 mm × 5.5 mm) with three different surface textures were implanted into the lateral distal femur as a part of another study examining bone ingrowth (not presented here). The animals were sacrificed 8 weeks after the first injection. Six pairs of femurs, tibiae, and humeri were selected to evaluate the structural and morphological changes of the bone caused by carrageenan knee arthritis and that of ten animals were used for mechanical evaluation.

2.2. Evaluation of the knee joint

The appearance of intraarticular structures, including the joint fluid, synovium, ligaments, menisci, and the soft tissue structures surrounding the knee joint, were observed. The degree of articular surface involvement of the patella, femur and tibia was classified under a dissection microscope according to the grading by Sommerlath and Gillqist [13]: Grade 0 – normal cartilage; Grade 1 – fibrillation; Grade 2 – pannus and fibrillation; Grade 3 – superficial clefts; Grade 4 – deep localized clefts; Grade 5 – large defects; Grade 6 – complete loss of cartilage on the weight-bearing surface. Soft tissue samples of the periarticular structures, such as joint capsule, synovium, ligaments, or menisci, were fixed in 10% buffered formalin and the patella, distal femur, and upper tibia were decalcified in 15% aqueous formic acid, followed by dehydration serially in ethanol, embedded in paraffin, cut into 5 μm thick sections, and stained with HE. Sections were viewed under a light microscope for any inflammatory or destructive changes.

2.3. Radiographic bone-density measurements

Following harvesting and removal of all soft tissues, the bones were radiographed on a Faxitron radiographic machine (Field Emission Corporation, McMinnville, OR) to obtain high-resolution radiographic images. These images were then scanned into a computer and bone density was measured at different locations on the bone image using grey scale analysis with an image analysis program (Image 1.57, National Institutes of Health, Bethesda, MD). The epiphyseal locations measured were the medial femoral condyle, femoral head, central tibial plateau, lateral distal tibial trochlea, and humeral head epiphysis. The diaphyseal locations measured were mid-femoral diaphysis, tibial diaphysis at the junction of middle and distal one-thirds, and the humeral diaphysis at the junction of proximal three-fifths and the distal two-fifths. The larger the grey-level number, the greater the X-ray transmission and therefore less bone mass.

2.4. Evaluation of long-bone geometry

The length of the long bones as well as the periosteal and endosteal dimensions were calculated from the plain radiographs with a sliding electronic digital caliper, correcting for magnification. Using an electronic digital caliper, the periosteal and endosteal measurements were taken at the mid-shaft of the femur, junction of middle and distal one-third of the tibia, and the junction of the proximal three-fifths and distal two-fifth of the humerus. The internal dimensions of the bones were measured after the bone was sectioned transversely. Considered to be elliptical, the cross-sectional area of the long bones was calculated using the following equation [14]

$$A = \pi\,(ab - a'b')/4 \qquad (1)$$

where a and a' are external and internal anteroposterior diameters of the long bones, respectively, and b and b' are external and internal mediolateral diameters. Selected femoral samples were defatted using 3% sodium hypochlorite overnight to remove residual soft tissue and marrow contents. The samples were then dehydrated in serial ethanol followed by critical point drying and gold sputter coating, and the inner surfaces were then viewed in a scanning electron microscope (SEM; Jeol 350, Jeol Ltd, Tokyo, Japan). Also, selected diaphyseal samples were dehydrated in serial ethanol, embedded in Spurr's embedding media, and 50 μm thick ground sections made. Sections were then stained with ethylene blue and viewed under light microscope.

2.5. Morphometric analysis of trabecular bone structure

Samples of epiphysis were cut and ground to a specific level (Table I) and underwent preparation for SEM examination. The SEM images were then scanned into the computer for morphometrical analyses. Trabecular bone volume (TBV; trabecular surface area divided by the total area in mm^2) was measured using NIH Image 1.57. The following parameters of cancellous bone were analysed manually using a square grid based on the SEM images: (1) Tb.N was defined as the average number of trabecular elements encountered per unit area; 2) Ho.N was defined as the average number of holes per unit area; (3) a Euler number was calculated by deducting Ho.N from Th.N [15]; (4) Tb.Th was defined as the average thickness of trabeculae; and (5) Tb.Sp was defined as the average distance between trabeculae, which represents the amount of marrow space [16].

Trabecular nodes (Nd) and free ends or termini (Tm) were analysed according to the method given by Mellish *et al.* [17]. An Nd was defined as a point where three trabecular struts intersected, and a Tm was defined as the terminus of a trabecular strut. The number of Tm and Nd per unit area (Nd/mm^2 and Tm/mm^2) and the ratio of Nd/Tm were measured and calculated. Also, the thickness of the subchondral bone plate (SCBP) was measured at five points on the joint surface with an equal distance in between and the mean of the five measurements was calculated.

TABLE I Surfaces or sections created for morphometrical evaluation

Bone	Method	Surface created for indentation test
Femoral head	SEM image	Cut and ground from anterior side to a depth of 30% of the whole thickness.
Fem. condyle (medial)	Ground section[a]	A horizontal plane 5–6 mm from the lowest point of the joint surface, in which the implant was included.
Upper tibial epiphyses	SEM image	Cut and ground from anterior side to a depth of one-third of the whole thickness.
Distal tibial epiphysis	SEM image	Cut and ground from anterior side to a depth of 50% of the whole thickness.
Humeral head	SEM image	Cut and ground from posterior side to a depth of 40% of the whole thickness.

[a] The ground sections for evaluating bone ingrowth to implants were used for the morphometrical analysis of medial femoral condyle. Briefly, the image was photographed, scanned into computer, and analysed in the same way used for the other bones.

2.6. Mechanical testing

The mechanical testing methods have been described previously [18]. Briefly, the test machine (MTS System 810, Minneapolis, MN) was operated in a displacement control mode with a ramp function for both three-point bending and indentation tests. The machine displacement transducer had been previously calibrated using an extensometer. The load versus displacement was recorded using a chart recorder. Load at the highest point of the curve was taken as the maximum load recorded during the test. A stiffness measure of either diaphyseal bone (bending stiffness) or cancellous bone (indentation stiffness) was obtained by measuring the slope of the linear portion on the load–displacement curves.

For the three-point bending tests, the long bones were stripped of all soft tissues. The point to be tested was located and marked and dimensions at that point were measured with a sliding electronic caliper. After the bone was positioned on the two metal supports of the testing gear (6 mm diameter each and a 50 mm span) and the upper loading striker (6 mm diameter) was adjusted close enough to the specimen surface, the striker was driven to the bone surface at a constant rate of $1.0\,\mathrm{mm\,min^{-1}}$ until fracture. The surface of bone facing the loading striker was posterior for the femur, anterior for the tibia, and lateral for the humerus. The breaking point was chosen at the mid-shaft of the femur, junction of middle and distal one-thirds of tibia, and junction of the proximal three-fifths and distal two-fifths of the humerus. The specimen aspect ratios (length to width) in this experimental setting were 6.25 for the femur, 8.67 for the tibia and 7.62 for the humerus. During preparation and testing the samples were kept moist with saline. The following equation was used for calculating the ultimate bending strength (or ultimate stress) [18]

$$\sigma_b = P_b L a / 8I \tag{2}$$

where P_b is the ultimate load, a is the average value of the external anteroposterior diameters of the cross-sections at the loading point of the bone, L is the distance between the supporting bars (equal to the length of bone tested), and I is the area moment of inertia which was calculated assuming the long-bone cross-sections (both outer circumference and the shape of medullary canal) to be elliptical tubular [14, 18]

$$I = \pi(a^3 b - a'^3 b')/64 \quad \text{(for femur and tibia)} \tag{3}$$

$$I = \pi(a b^3 - a' b'^3)/64 \quad \text{(for humerus)} \tag{4}$$

The values chosen for a, a', b and b' are the average values of the external and internal anteroposterior and mediolateral diameters of the cross-sections at the loading points of the bone. The remainder of the tested portion of the bone was assumed to be consistent in cross-sectional size and shape. For the humerus, Equation 4 was used, because the surface of bone facing the loading striker was lateral for humerus. The external diameters (a and b) were measured before mechanical testing using an electronic digital caliper. After testing, the pieces were glued together and sectioned transversely at the loading point. The dimensions of the medullary canal (a' and b') were then measured. The following equation was used for calculating the Young's modulus of the diaphyseal bones [18]

$$E_b = SL^3/48I \tag{5}$$

where S is the bending stiffness and L is the distance between the supporting bars (equal to the length of bone tested).

For indentation testing, selected sample bones were cut on a bandsaw and then ground on a rotating grinder to a certain depth in the cancellous bone of the epiphysis (Fig. 1). The platform holding the specimen was levelled to ensure that all loading was perpendicular to the specimen surface. A cylindrical stainless steel indentor 2.8 mm diameter with a flat bone-contacting surface was used. After the specimen was positioned on the platform and the indentor adjusted close to the

Figure 1 Bone surfaces created for the indentation test. Femoral head: ground from the anterior side to a depth of 30% of the whole thickness. Tibial plateau: ground from the anterior side to a depth of one-third of the whole thickness. Humeral head: ground from posterior side to a depth of 30% of the whole thickness.

specimen surface, the indentor was driven into the bone at a rate of 1 mm min^{-1}. The loading was stopped when the curve turned downward after the ultimate load. The ultimate load from each curve was divided by the indentor face area to obtain ultimate strength using the following formulae [18]

$$\sigma_i = 4\,P_i/\pi d^2 \quad (6)$$

where P_i is the ultimate indentation load and d is the diameter of the indentor.

2.7. Data analysis

Because most of the comparisons were between paired sample groups, they were analysed using the paired student T test, and significance was defined as $P < 0.05$. Pearson correlation coefficients were calculated between mechanical data by the indentation testing and morphologic parameters.

3. Results

3.1. Weight loss and inflammatory arthritis

By the time of sacrifice (8 weeks after the first injection and a total of 11 injections in 6 weeks), 18 animals lost weight, 6 stayed the same, and 10 gained weight. The mean weight before the injections was 3.89 ± 0.40 kg and at sacrifice 3.80 ± 0.49 kg. Thus, the weight loss was $2.1\% \pm 9.5\%$. If compared to a projected weight increase rate for rabbits without carrageenan injection over 8 weeks, which is $10.5\% \pm 8.2\%$ (calculation based on 99 rabbits from a previous study), the true weight loss was 12.6%.

After the first or second injection, most of the rabbits started to use their right legs less. The right knees became swollen, tender, and erythematous. These signs became more and more serious with the increasing number of injections. When the skin was cut during the necropsy, inflamed synovium and excessive joint fluid was evident. Most of the cruciate ligaments were swollen and lost their shiny appearance. Nearly all of the menisci were worn (thinner or smaller) and some of them were torn or separated longitudinally or horizontally. According to the grading of Sommerlath and Gillqist [13], nearly all of the joint surfaces (femoral, tibial, and patellar) were graded at least 3, with local superficial clefts or deep localized clefts on the cartilage surface. Histological sections showed severe inflammatory changes in the synovium and destruction of the articular surfaces.

3.2. Radiographic bone density

Comparisons of bone density for both cortical and cancellous bone are given in Table II. Significant differences were found for bone density between the left and right side for the femur and tibia but not the humerus.

3.3. Morphological changes of diaphyseal bone

In general, the femur and tibia showed obvious differences in cortical thickness, cross-sectional cortical bone area (CBA), and medullary canal area (MCA) between the right and left legs by direct measurement (Table III). No difference was found for the humerus. Statistical differences were also found between the bone length for the femur and tibia, although the difference was small (Table III). Although there were no statistically significant differences in the external diaphyseal dimensions, there was a trend for the right side of both the femur and tibia to be smaller. However, the cortical thickness was significantly less on the arthritic side. SEM showed different morphology of the endosteal surfaces between the arthritic and control side. For the femur, on the arthritic side in the proximal diaphysis the trabecular portion of the cortex was diminished and looked more porous, with thinner trabeculae. In the distal diaphysis of the femur, the endosteal surfaces were more porous than the control side and many cavities were seen on the cortical sectional surface, indicating subendosteal cavitation (Fig. 2). The ground sections of diaphyseal bones showed that for femur and tibia on the arthritic side, the endosteal surfaces were more porous than the control side and many cavities were seen (Fig. 3a–d). No similar changes were found for humerus (Fig. 3e, f).

3.4. Morphological changes of cancellous bone

In general, the femur and tibia showed obvious differences in cancellous bone structure between the right and left legs as shown by SEM (Fig. 4a–d). The TBV was significantly decreased for the right femur and

TABLE II Comparison of bone density[a]

Perimeter	Bone	N (pairs)	Control (left)	Arthritic (right)	P
Diaphyseal bone	Femur	10	151 ± 13	180 ± 11	< 0.001
	Tibia	10	150 ± 14	175 ± 12	< 0.001
	Humerus	10	140 ± 9	141 ± 10	0.751
Epiphyseal bone	Femoral head	10	109 ± 15	155 ± 18	< 0.001
	Medial fem. condyle	10	56 ± 30	118 ± 18	0.001
	Upper tibia	10	47 ± 14	85 ± 17	< 0.001
	Distal tibia	10	122 ± 9	163 ± 9	< 0.001
	Humeral head	10	88 ± 14	87 ± 13	0.742

[a]Bone density was measured as greylevel (range: 0–256) on high-resolution X-ray films (mean $\pm$ S.D.).

TABLE III Paired comparison of the parameters between left and right diaphyseal bones[a]

Perimeter	Bone	*N* (pairs)	Control (left)	Arthritic (right)	*P*
Bone length (mm)	Femur	36	101.63 ± 3.01	101.01 ± 3.35	0.003
	Tibia	24	108.57 ± 3.85	108.17 ± 3.61	0.008
	Humerus	23	76.38 ± 3.03	76.26 ± 3.06	0.392
Diaphyseal dimensions (mm)	Femur thickness	10	7.71 ± 0.31	7.64 ± 0.31	0.503
	Femur width	10	10.21 ± 0.52	10.05 ± 0.66	0.186
	Tibia thickness	10	5.85 ± 0.23	5.70 ± 0.28	0.200
	Tibia width	10	8.66 ± 0.44	8.59 ± 0.46	0.449
	Humerus thickness	10	6.50 ± 0.44	6.62 ± 0.42	0.310
	Humerus width	10	7.33 ± 0.39	7.29 ± 0.40	0.500
Cortical thickness (mm)	Tibial (a)[b]	10	1.22 ± 0.20	0.97 ± 0.18	< 0.001
	Tibial (b)[b]	10	1.55 ± 0.16	1.24 ± 0.16	< 0.001
	Femur	10	1.24 ± 0.24	0.89 ± 0.12	< 0.001
	Humerus	10	1.25 ± 0.15	1.24 ± 0.13	0.881
Cross-sectional cortical bone area (CBA) (mm^2)	Femur	10	29.81 ± 4.56	22.19 ± 2.95	< 0.001
	Tibia	10	24.80 ± 2.29	20.41 ± 2.71	0.003
	Humerus	10	22.08 ± 2.22	22.23 ± 2.83	0.830
Cross-sectional medullary bone area (MCA) (mm^2)	Femur	10	32.03 ± 6.46	38.24 ± 5.61	0.005
	Tibia	10	14.91 ± 1.75	18.06 ± 1.69	< 0.001
	Humerus	10	15.42 ± 3.96	15.73 ± 2.56	0.726

[a]Values are the mean ± S.D.
[b]Where (a) is the anterior and posterior cortical thickness and (b) is the medial and lateral cortical thickness. For femur and humerus, (a) and (b) were basically the same by gross, histological, and SEM evaluations.

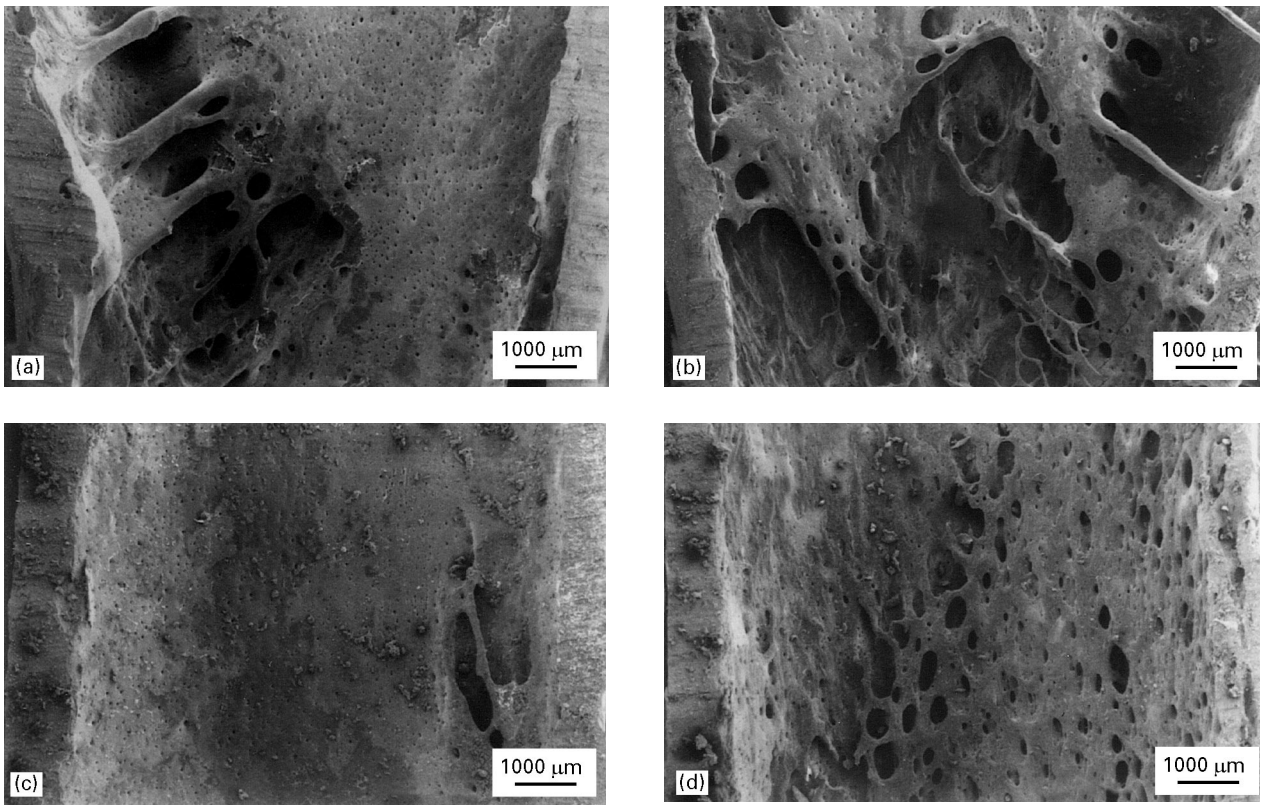

Figure 2 Morphological changes of the endosteal surface of the femoral diaphysis by SEM. On the arthritic side in the proximal diaphyseal region (b) the trabecular portion of the cortex was diminished and looked more porous, with obvious thinner trabeculae compared to the control side (a). At the distal one-third of the femur on the arthritic side (d) the endosteal surfaces were more porous than the control side (c) and many cavities were seen on the cortical sectional surface (d), which indicated subendosteal cavitation.

tibia (Table IV). The trabeculae on the right side were thinner and had wider marrow spaces. The subchondral bone plate was also much thinner on the arthritic side. No obvious differences were found for the humerus (Table IV, Fig. 4e, f). All the indices in Table V show less connectivity on the arthritic side for the femur and tibia compared to the control side, but not for the humerus.

3.5. Mechanical properties of the bone

Based on the bending test, the ultimate load, ultimate bending strength, and stiffness of the right femurs and tibias (arthritis side) were much lower than the contralateral left femurs and tibias (control side). The Young's modulus of femurs was lower for the right side than the left side, but not for the tibia. No differences for any of the parameters were found for humerus (Table VI). The effect of carrageenan-arthritis on the indentation properties of epiphyseal bones was analysed by indentation testing. The ultimate load, stiffness, and ultimate indentation strength of right femoral heads and proximal tibiae were much lower than the contralateral side. No differences were found for any of the parameters for humeral heads (Table VII). Good correlations were revealed between the mechanical and morphometrical parameters (Table VIII).

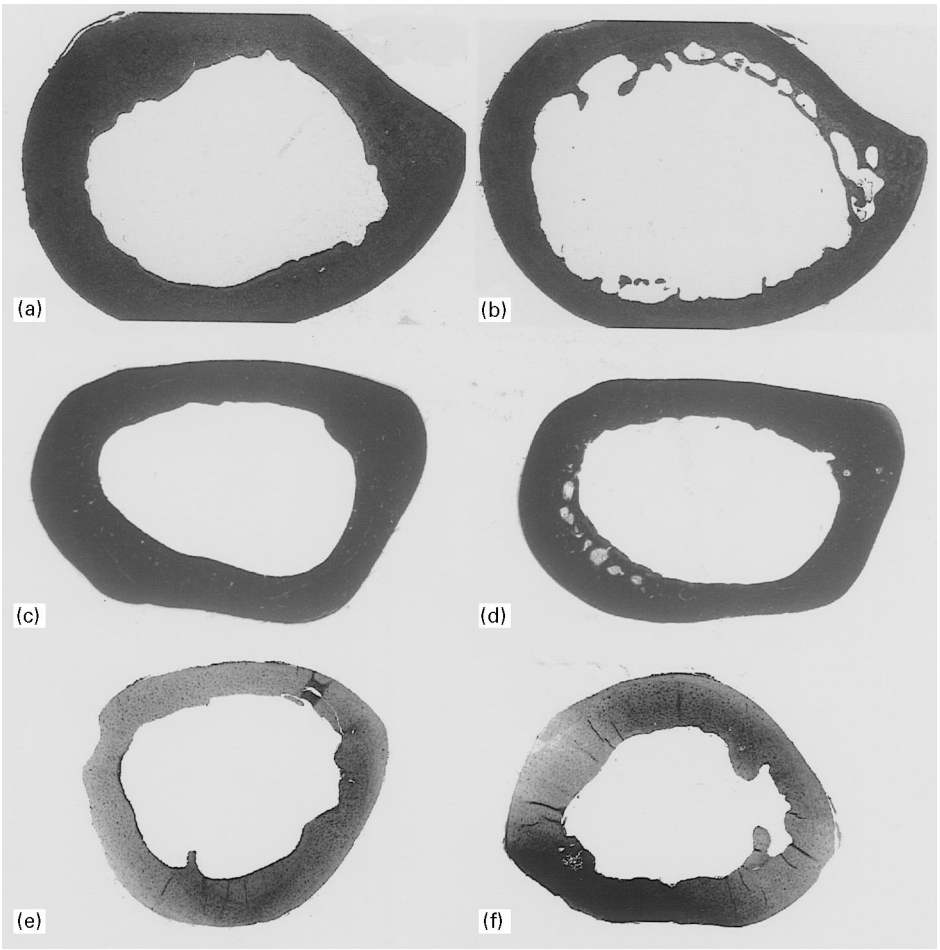

Figure 3 The ground sections (low power) of diaphyseal bones showed that for femur and tibia, on the arthritic side, the endosteal surfaces were more porous than the control side and many cavities were seen, which again indicated subendosteal cavitation, (a) left femur, (b) right femur, (c) left tibia, (d) right tibia. The same changes were not found for humerus, (e) left, (f) right.

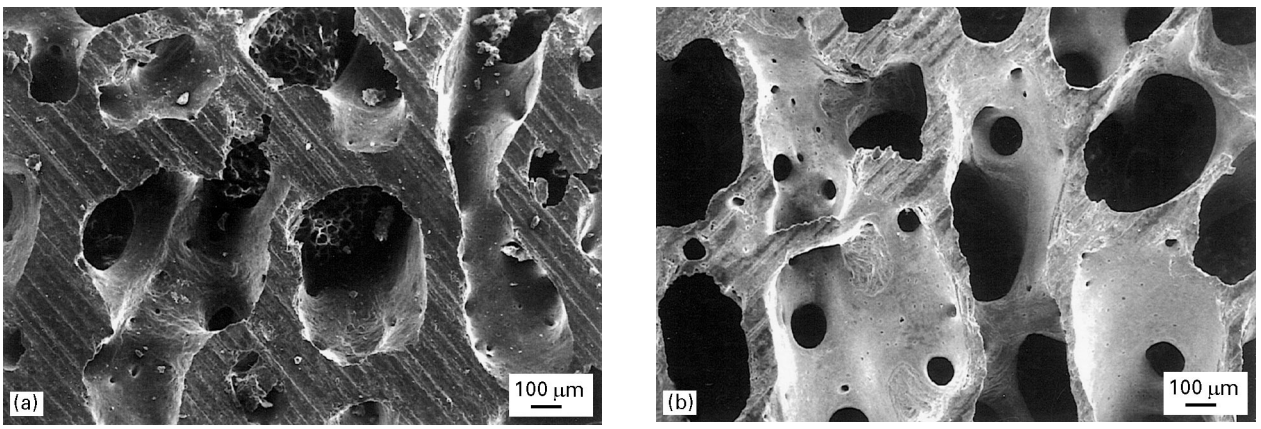

Figure 4 Morphological differences between the arthritic side and control side of femoral head epiphysis by SEM. The obvious findings included the much thinner trabecular and bigger marrow spaces for the femoral head, (a) left, (b) right and tibial plateau (c) left, (d) right, but not for the humeral head, (e) left, (f) right.

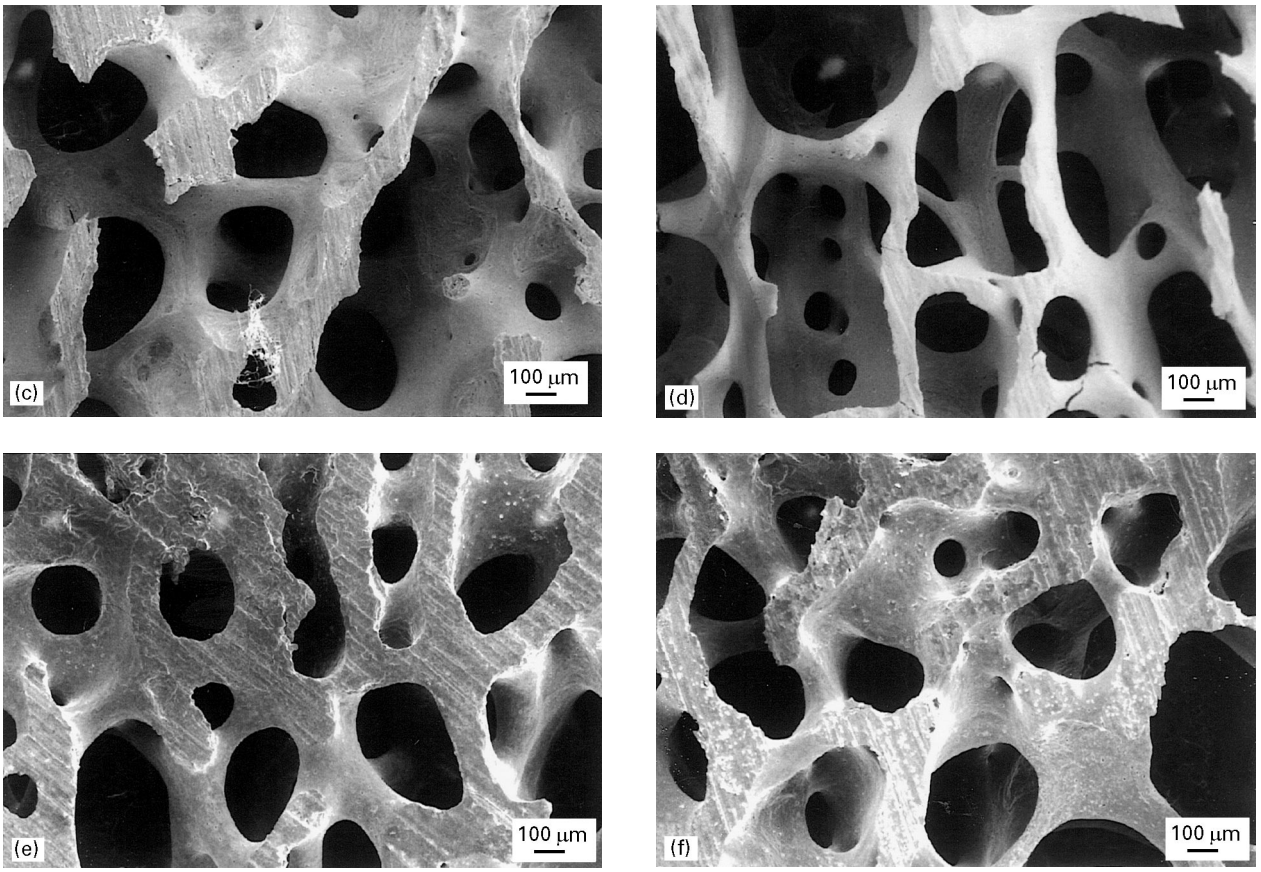

Figure 4 (Continued)

TABLE IV Paired comparison of trabecular structure between left and right epiphyseal bones[a]

Perimeter	Bone	*N* (pairs)	Control (left)	Arthritic (right)	*P*
TBV (%)	Femoral head	6	48 ± 11	28 ± 3	0.003
	Medial femoral condyle	6	35 ± 7	19 ± 6	0.001
	Upper tibia	6	30 ± 6	16 ± 6	< 0.001
	Distal tibia (lat. trochlea)	5	45 ± 11	26 ± 10	0.023
	Humeral head	6	37 ± 10	33 ± 3	0.429
Tb.Th (μm)	Femoral head	6	238 ± 66	110 ± 27	0.004
	Medial femoral condyle	6	149 ± 21	92 ± 8	0.001
	Upper tibia	6	163 ± 40	122 ± 28	0.018
	Distal tibia (lat. trochlea)	5	266 ± 54	161 ± 41	0.005
	Humeral head	6	147 ± 20	148 ± 21	0.979
Tb.Sp (μm)	Femoral head	6	287 ± 72	404 ± 75	0.013
	Medial femoral condyle	6	342 ± 95	427 ± 61	0.015
	Upper tibia	6	355 ± 68	476 ± 87	0.004
	Distal tibia (lat. trochlea)	5	359 ± 95	548 ± 173	0.025
	Humeral head	6	339 ± 36	323 ± 22	0.301
Subchondral bone plate (SCBP) (μm)	Femoral head	6	500 ± 100	310 ± 100	0.044
	Medial femoral condyle	6	354 ± 51	143 ± 48	0.009
	Upper tibia	6	350 ± 260	280 ± 280	0.039
	Distal tibia (lat. trochlea)	5	780 ± 200	570 ± 130	0.005
	Humeral head	6	320 ± 40	340 ± 40	0.282

[a]Values are the mean ± S.D.

4. Discussion

4.1. Inflammatory arthritis

Carrageenan injection induced a very strong inflammatory arthritis which was very severe after only a few injections, usually within 1 or 2 weeks. It not only resulted in severe osteopenia of the adjacent long bones, but affected the animal systematically as shown by a significant weight loss in only 8 weeks. This agrees with the findings of Bogoch *et al.* [1] that this animal model is appropriate for studying bone remodelling in inflammatory arthritis, because it reliably reproduces the morphological changes of inflammatory arthritis seen in both the periarticular soft tissues and adjacent bones.

TABLE V Comparison of cancellous bone connectivity between left and right epiphysis[a]

Perimeter	Bone	*N* (pairs)	Control (left)	Arthritic (right)	*P*
CTBE/mm^2	Femoral head	6	0.29 ± 0.01	0.94 ± 0.77	0.090
	Lateral femoral condyle	5	0.75 ± 0.44	1.35 ± 0.19	0.030
	Upper tibia	6	1.07 ± 0.50	1.82 ± 0.77	0.109
	Distal tibia (lateral trochlea)	5	0.47 ± 0.26	1.21 ± 0.80	0.065
	Humeral head	6	0.94 ± 0.55	1.35 ± 0.77	0.348
Ho.N/mm^2	Femoral head	6	2.46 ± 1.08	1.25 ± 0.51	0.012
	Lateral femoral condyle	5	2.09 ± 0.50	0.90 ± 0.11	0.008
	Upper tibia	6	1.22 ± 1.01	0.52 ± 0.54	0.109
	Distal tibia (lateral trochlea)	5	2.26 ± 1.20	0.59 ± 0.41	0.009
	Humeral head	6	1.70 ± 1.09	1.47 ± 0.54	0.438
Nd/mm^2	Femoral head	6	3.27 ± 1.09	2.01 ± 0.53	0.022
	Lateral femoral condyle	5	2.38 ± 0.40	1.74 ± 0.43	0.045
	Upper tibia	6	2.20 ± 1.68	1.15 ± 1.33	0.017
	Distal tibia (lateral trochlea)	5	2.61 ± 1.13	1.14 ± 0.56	0.009
	Humeral head	6	2.36 ± 0.73	2.08 ± 0.72	0.100
Tm/mm^2	Femoral head	6	0.51 ± 0.26	2.16 ± 1.27	0.063
	Medial femoral condyle	6	2.11 ± 0.83	3.87 ± 0.35	0.015
	Upper tibia	6	2.03 ± 0.99	3.10 ± 1.18	0.016
	Distal tibia (lateral trochlea)	5	0.98 ± 0.45	2.20 ± 0.93	0.038
	Humeral head	6	1.83 ± 0.68	2.65 ± 0.70	0.025
Euler number[b]	Femoral head	6	− 2.16 ± 1.08	− 0.31 ± 1.12	0.048
	Lateral femoral condyle	5	− 1.34 ± 0.62	0.74 ± 0.31	0.006
	Upper tibia	6	− 0.15 ± 1.30	1.30 ± 1.14	0.035
	Distal tibia (lateral trochlea)	5	− 1.79 ± 1.06	0.63 ± 0.83	0.005
	Humeral head	6	− 0.75 ± 1.49	− 0.12 ± 0.69	0.227
Nd/Tm	Femoral head	6	8.36 ± 5.45	1.36 ± 1.14	0.037
	Lateral femoral condyle	5	1.29 ± 0.54	0.45 ± 0.09	0.021
	Upper tibia	6	3.43 ± 1.35	0.39 ± 0.37	0.090
	Distal tibia (lateral trochlea)	5	2.85 ± 1.13	0.59 ± 0.33	0.011
	Humeral head	6	1.64 ± 1.14	0.81 ± 0.25	0.138

[a]Values are the mean ± S.D.
[b]Euler number = (number of continuous bone elements − number of holes)/mm^2.

TABLE VI Effect of carrageenan-arthritis on bending property (by three-point bending) of rabbits long bones (n = 10 pairs/each bone)[a]

Bones	Ultimate Load (N)	Stiffness (N mm^{-1})	Ultimate strength (MPa)	Young's modulus (GPa)
Femoral diaphysis				
Left	380 ± 65	604 ± 83	97 ± 21	8.3 ± 1.5
Right	227 ± 33	370 ± 51	80 ± 16	7.1 ± 1.4
P Value	< 0.001	< 0.001	0.008	0.016
Tibial diaphysis				
Left	395 ± 39	474 ± 72	186 ± 26	15.9 ± 2.9
Right	299 ± 41	353 ± 70	173 ± 19	14.9 ± 2.2
P Value	< 0.001	< 0.001	0.054	0.377
Humeral diaphysis				
Left	350 ± 39	461 ± 76	158 ± 25	11.9 ± 2.7
Right	349 ± 33	473 ± 48	157 ± 26	12.4 ± 2.4
P Value	0.918	0.625	0.845	0.904

[a]Values are the mean ± S.D.

4.2. Changes of bone morphology and structure

With the rapid development of image analysis programs, direct measurements of bone density on high-resolution radiographs becomes straightforward. The data from this study showed decreased bone density of the long bones on the arthritic side. The reason for the density decrease is the reduced bone volume, both for cortical and cancellous bone, as shown by morphological evaluation and morphometrical analysis. As shown by the paired comparison of the bone indices, the structural changes of both cortical and cancellous bone on the arthritic side were significant. Reduced bone volume and increased marrow space (i.e. decreased TBV and CBA, and increased Th.Sp and MCA) are the predominant changes documenting

the osteopenia. These changes are similar to those found in most osteoporotic conditions such as osteoporosis of rheumatoid arthritis [19–21], senior osteoporosis [22], and traumatic osteodystrophy [23].

Aside from the reduction in bone volume and increase in marrow space, the qualitative three-dimensional trabecular network changes such as trabecular connectivity may be more significant [15, 24]. Connectivity in cancellous bone is a three-dimensional characteristic of the trabecular network. It describes the presence of multiple connections between trabeculae. On a two-dimensional section, trabecular elements can be described as nodes and struts with two free ends. The more nodes per unit area, the more connections in the trabecular network. The more free struts present, the fewer connections between trabeculae.

A high Nd/Tm ratio means more connections between trabeculae. Another useful index for connectivity is a Euler number, which is a topological property based on the number of connected trabecular elements (Th.N) and holes (Ho.N) in a given section. An Euler number is determined by deducting Ho.N from Th.N. Cancellous structures with high connectivity, as in young adults, have a high negative Euler number, while in bone from older subjects or patients with osteoporosis, the value will be a smaller negative or positive number. In the carrageenan-induced arthritic knees, adjacent bones showed obvious perforation and disconnectivity in a very short period of time as indicated by the Nd/Tm ratio of Euler number, which represents a rapid loss of bone [16], featuring perforation and disconnection of the trabecular network and increased size of marrow cavities, as is seen in post-menopausal osteoporosis [22] or the early stages of osteoporosis that occur after corticosteroid administration, traumatic osteodystrophy, or immobilization [23, 25]. This kind of bone loss in cortical bones leads to subendosteal cavitation and conversion of the inner portion of the cortex to a trabecular-like structure, which then undergoes the same changes as the trabecular bone originally present [16, 26]. Subendosteal cavitation and conversion of the inner portion of the cortex to a trabecular-like structure was indeed found in this model (Fig. 3). Rapid bone loss is an osteoclast-mediated process [16, 26]. Bogoch *et al.* found a much faster bone resorption than osteogenesis in an inflammatory arthritis model [1, 2]. Another important feature of the rapid bone loss is the dramatically reduced bone strength, which has been demonstrated by mechanical analysis in this study.

TABLE VII Effect of carrageenan-arthritis on mechanical property (by indentation test) of rabbits epiphyseal bones ($n = 10$ pairs/each part)[a]

Bones	Ultimate Load (N)	Stiffness (N mm^{-1})	Ultimate strength (MPa)
Femoral head			
Left	419 ± 90	2296 ± 1041	68 ± 15
Right	159 ± 48	1038 ± 704	26 ± 8
P Value	< 0.001	0.006	< 0.001
Upper tibial			
Left	207 ± 50	1232 ± 469	34 ± 8
Right	100 ± 45	565 ± 298	16 ± 7
P Value	< 0.001	< 0.001	< 0.001
Humeral head			
Left	183 ± 47	1397 ± 724	30 ± 8
Right	184 ± 52	1179 ± 849	30 ± 8
P Value	0.933	0.411	0.934

[a]Values are the mean ± S.D.

4.3. Causes of osteopenia

The exact cause of the osteopenic changes remains unclear. Bogoch *et al.* reported that carrageenan arthritis caused increased new bone volume in the controlateral femur and ipsilateral humerus [4]. Interleukin 1 and prostaglandin E have been shown to stimulate bone resorption [27]. The increased amount of such local factors may contribute to the development of periarticular osteopenia. However, this does not explain what causes the osteopenia at locations away from the arthritic knee, such as the femoral head and distal tibia. The juxtaarticular bone loss may also be explained by changes in local blood flow due to increased intraarticular pressure [10] and the presence of a joint effusion [11] resulting from the arthritis. However, this does not explain the bone loss distant from the arthritic knee, because these factors are localized and not systemic, and are not likely to have any effect on the circulation in remote locations.

Bone mass is known to decrease in the absence of stimulation from gravity or weight-bearing ambulation [6–9], which may play an important role in this model. This theory is supported by the results from this study. As early as 1–2 weeks after the inflammatory arthritis developed, the rabbits used their right legs less and less and some of them even carried their

TABLE VIII Correlation analysis (Pearson correlation coefficient) between mechanical and morphometric parameters[a]. Minus signs indicate negative correlation

	TBV (%)	Tb.Th (μm)	Tb.sp (μm)	CTE (mm^{-2})	Ho.N (mm^{-2})	Euler number (mm^{-2})	Nd (mm^{-2})	Tm (mm^{-2})	Nd/Tm ratio
Ultimate load	0.796[b]	0.918[c]	− 0.459	0.767[b]	0.823[b]	− 0.832[b]	0.868[b]	− 0.879[b]	0.940[d]
Ultimate stiffness	0.888[c]	0.869[b]	− 0.562	0.824[b]	0.880[b]	− 0.892[b]	0.950[d]	− 0.925[c]	0.831[c]
Ultimate strength	0.796	0.918[c]	− 0.462	0.769[b]	0.823[b]	− 0.883	0.869[b]	− 0.881[b]	0.940[d]

[a]$n = 6$; degrees of freedom $n' = n - 2 = 4$; one way (for positive r) or two way (negative r) analysis.
[b]$P < 0.05$.
[c]$P < 0.01$.
[d]$P < 0.005$.

legs. Osteopenia was found not only in the juxta-articular bones but also in locations away from the knee, such as the femoral head and distal tibia of the same limb. All of these locations are subject to the effects of disuse, while the contralateral femur, tibia and both humerus, which are not affected by disuse, had no osteopenic changes.

4.4. Mechanical properties of the bone

Very little data of the mechanical properties of rabbit bones can be found in the literature. One report on elastic modulus of rabbit tibiae tested by the ultrasonic method [28] gave an elastic modulus of 19.0 GPa, which is in the range of diaphyseal bones of other species. Simple parameters, such as yield strength [29] or peak load [30] of the rabbit tibia were reported, but the data cannot be used for comparison with other studies. The current study performed a standardized three-point bending test for rabbit long bones and ultimate load, stiffness, ultimate strength, and elastic modulus were documented (Table II). For example, the elastic modulus of rabbit tibia is 15.9 ± 2.9 GPa, which is in the range (5–21 GPa) for diaphyseal bone of other species [31]. According to the data in Table VI, the ultimate load for femur and tibia are basically the same, but the ultimate strength and elastic modulus are very different. This could be explained by their different geometric structure, because the femur is bigger in overall diameter than the tibia.

Mechanical properties of a whole diaphyseal bone depend on both the quantity and quality of bone tissue [16, 32]. Based on this study, thinning of the diaphyseal cortex is the main structural basis for the diminished mechanical strength. Significant differences in cross-sectional area between the arthritic and control sides have been found in this study. Increased subendosteal porosity or cavitation is also likely to weaken the bone [16, 32]. If the differences of ultimate load and stiffness were caused by the reduced cross-sectional area of long bones (bone volume), then the difference of elastic modulus and ultimate bending strength should be caused by the diminished bone quality (porous change of endosteal bone). It is noted that the decreased elastic modulus of diaphyseal bones (14% for diaphyseal femur) was not as much as that of the cancellous bone (49% for femoral head).

4.5. Mechanisms of the reduced mechanical strength

In cortical bone, the bone loss leads to subendosteal cavitation and conversion of the inner portion of the cortex to a trabecular-like structure, which then undergoes the same changes as the trabecular bone originally present [16]. Subendosteal cavitation and conversion of the inner portion of the cortex to a trabecular-like structure was indeed found in this model. Rapid bone loss is an osteoclast-mediated process [16], as the results from Bogoch *et al.* [1, 2] seem to confirm. They found a much faster bone resorption rate than osteogenesis in an inflammatory arthritis model. An important feature of the rapid bone loss is the dramatically reduced bone strength, which has been demonstrated by the morphologic and mechanical data in this study.

The significant reduction of cancellous bone strength could be explained by the reduction of trabecular bone volume (TBV) and increased perforation and disconnectivity of the trabecular tissue. According to morphometrical analysis, the cancellous bones showed obvious perforation and disconnectivity in a very short period of time, as indicated by TBV, trabecular node (Nd), free end (Tm), continuous trabecular element (CTE), medullary holes (Ho.N), Nd/Tm ratio, and Euler number. These changes may represent a rapid bone loss [16] featuring perforation and disconnection of the trabecular network and increased size of marrow cavities. Significant correlations have been found between the mechanical and morphological parameters, and the data in Table VIII indicate both bone volume and quality play important roles in the dramatically reduced bone strength.

5. Conclusions

1. The carrageenan-induced knee arthritis resulted in osteopenic changes to the entire ipsilateral femur and tibia, including the femoral head and distal tibia, but not the contralateral femur and tibia and the remote humerus.
2. The carrageenan arthritis caused a dramatic decrease of bone strength to the entire ipsilateral femur and tibia, including the femoral head and distal tibia, but not the contralateral femur and tibia and the remote humerus.
3. The structural changes in bone volume and quality are the basis for the reduced mechanical strength. These results demonstrate that this rabbit model can be used as a model for studying localized osteopenia.

Acknowledgements

The authors are grateful to Drs R. A. Draughn and R. A. Young, Department of Materials Science, Dental School, MUSC, for technical consultation and instruction on mechanical testing. The work was partially supported by a grant from Osteonics, Inc.

References

1. E. R. BOGOCH, N. GSCHWEND, B. BOGOCH, B. RAHN and S. PERREN, *J. Orthop. Res.* **6** (1988) 648.
2. *Idem*, *Arthritis Rheum.* **32** (1989) 617.
3. *Idem*, *J. Orthop. Res.* **11** (1993) 292.
4. E. R. BOGOCH, E. MORAN, S. CROWE and V. FORNASIER, *ibid.* **13** (1995) 777.
5. K. SØBALLE, C. M. PEDERSEN, A. ODGAARD, G. I. JUHL, E. S. HANSEN, H. B. RASMUSSEN, I. HVID and C. BÜNGER, *Skeletal Radiol.* **20** (1991) 345.
6. V. S. SCHNEIDER and J. McDONALD, *Calcif. Tiss. Int.* **36** (1984) S151.
7. G. D. WHEDON, *ibid.* **36** (1984) S146.
8. T. J. WRONSKI and E. R. MOREY, *Clin. Orthop.* **181** (1983) 269.
9. D. R. YOUNG, W. J. NIKLOWITZ, R. J. BROWN and W. S. S. JEE, *Bone* **7** (1986) 109.

10. E. S. HANSEN, K. SØBALLE, T. B. HENRIKSEN, V. E. HJORTDAL and C. BÜNGER, *J. Orthop. Res.* **9** (1991) 191.
11. C. BÜNGER, *Acta Orthop. Scand.* **58** (Suppl 222) (1987) 1.
12. D. L. GARDNER, *Ann. Rheum.* **19** (1960) 369.
13. K. SOMMERLATH and J. GILLQIST, *Amer. J. Sports. Med.* **20** (1992) 73.
14. Z. Q. PENG, J. TUUKKANEN and H. K. VÄÄNANEN, *J. Bone Miner. Res.* **9** (1994) 1559.
15. J. E. COMPSTON, *Bone* **15** (1994) 463.
16. A. M. PARFITT, *Calcif. Tiss. Int.* **36** (1984) S123.
17. R. W. E. MELLISH, M. W. FERGUSON-PELL, G. V. B. COCHRAN, R. LINDSAY and D. W. DEMPSTER, *J. Bone Miner. Res.* **6** (1991) 689.
18. Y. H. AN, Q. KANG and R. J. FRIEDMAN, *Amer. J. Vet. Res.* **57** (1996) 1786.
19. A. C. KENNEDY and R. LINDSAY, *Clin. Rheum. Dis.* **3** (1977) 403.
20. P. D. SAVILLE, *Arthritis Rheum.* **10** (1967) 423.
21. S. SHIMIZU, S. SHIOZAWA, K. SHIOZAWA, S. IMURA and T. FUJITA, *ibid.* **28** (1985) 25.
22. R. G. CRILLY, A. HORSMAN, D. H. MARSHALL and B. E. C. NORDIN, *Front Hormone Res.* **5** (1978) 53.
23. P. MINAIRE, P. MEUNIER, C. EDOUARD, J. BERNARD, P. COURPRON and J. BOURRET, *Calcif. Tiss. Res.* **17** (1974) 57.
24. S. A. GOLDSTEIN, R. GOULET and D. MCCUBBREY, *ibid.* **34** (1993) S127.
25. D. W. DEMPSTER, M. D. ARLOT and P. J. MEUNIER, *ibid.* **34** (1982) S4.
26. A. M. PARFITT, C. H. E. MATHEWS, A. R. VILLANUEVA, M. KLEEREKOPER, B. FRAME and D. S. RAO, *J. Clin. Invest.* **72** (1983) 1396.
27. T. J. CHAMBERS, *Clin. Orthop.* **151** (1980) 283.
28. S. LEES and D. B. HANSON, *Calcif. Tiss. Int.* **50** (1993) 88.
29. R. WOOTTON, P. JENNINGS, C. KING-UNDERWOOD and S. J. WOOD, *Int. Orthop.* **14** (1990) 189.
30. T. J. NASH, C. R. HOWLETT, C. MARTIN, J. STEELE, K. A. JOHNSON and D. J. HICKLIN, *Bone* **15** (1994) 203.
31. J. D. CURREY, *J. Biomech.* **21** (1988) 131.
32. D. R. CARTER, W. C. HAYES, D. J. SCHURMAN, *ibid.* **9** (1976) 211.

Received 19 May
and accepted 16 September 1997